

## **Accelerator/Experiment Operations - FY 2014**

P. Czarapata, S. Geer<sup>1</sup>, D. Geesaman, D. Harris, K. Lang, K. McFarland, C. D. Moore, S. Nagaitsev, R. Plunkett, P. Reimer, J. J. Schmidt, A. K. Soha, R. Tayloe, J. Thomas, D. Torretta, R. Van de Water

This Technical Memorandum (TM) summarizes the Fermilab accelerator and accelerator experiment operations for FY 2014. It is one of a series of annual publications intended to gather information in one place. In this case, the information concerns the FY 2014 MINOS and MINERvA experiments using the Main Injector Neutrino Beam (NuMI), the MiniBooNE experiment running in the Booster Neutrino Beam (BNB), and the SeaQuest experiment and Meson Test Beam (MTest) activities in the 120 GeV external Switchyard beam (SY120).

Each section was prepared by the relevant authors, and was somewhat edited for inclusion in this summary.

### **Accelerator Operations** (Sergei Nagaitsev, Paul C. Czarapata)

#### *FY 2014 Accelerator Operations*

The low-energy and high-energy neutrino beams, the SeaQuest beam, and the Test Beams in the Meson area were brought into operation after the modifications for the NOvA (ANU) upgrades. The high-energy neutrino beam was scheduled for beam delivery for 48 weeks. The startup occurred on October 7<sup>th</sup> and ran until the present shutdown which began September 5<sup>th</sup> for Muon Campus, PIP, and Recycler work. The total hours of high-energy operation were 7125.4.

Booster Neutrino beam was scheduled for 46 of the 52 week time period. BNB beam was delivered starting on October 21<sup>st</sup>. During this period the number of booster cavities refurbished and installed was 14. Two cavities subsequently failed due to hidden manufacturing defects from their initial construction over forty years earlier. Work on the PIP program continues on pace. The total hours of beam delivered were 7076.8.

SeaQuest was scheduled for beam delivery for 44 weeks. The starting date for beam delivery was November 4<sup>th</sup>. The main reason for the delay in startup was the continuing vacuum problems in the 30+ year old transport line to the Neutrino area. Ultimately a sleeve of over 700ft was installed and beam transport began. Beam delivery time was 5150.4 with  $5.91 \times 10^{17}$

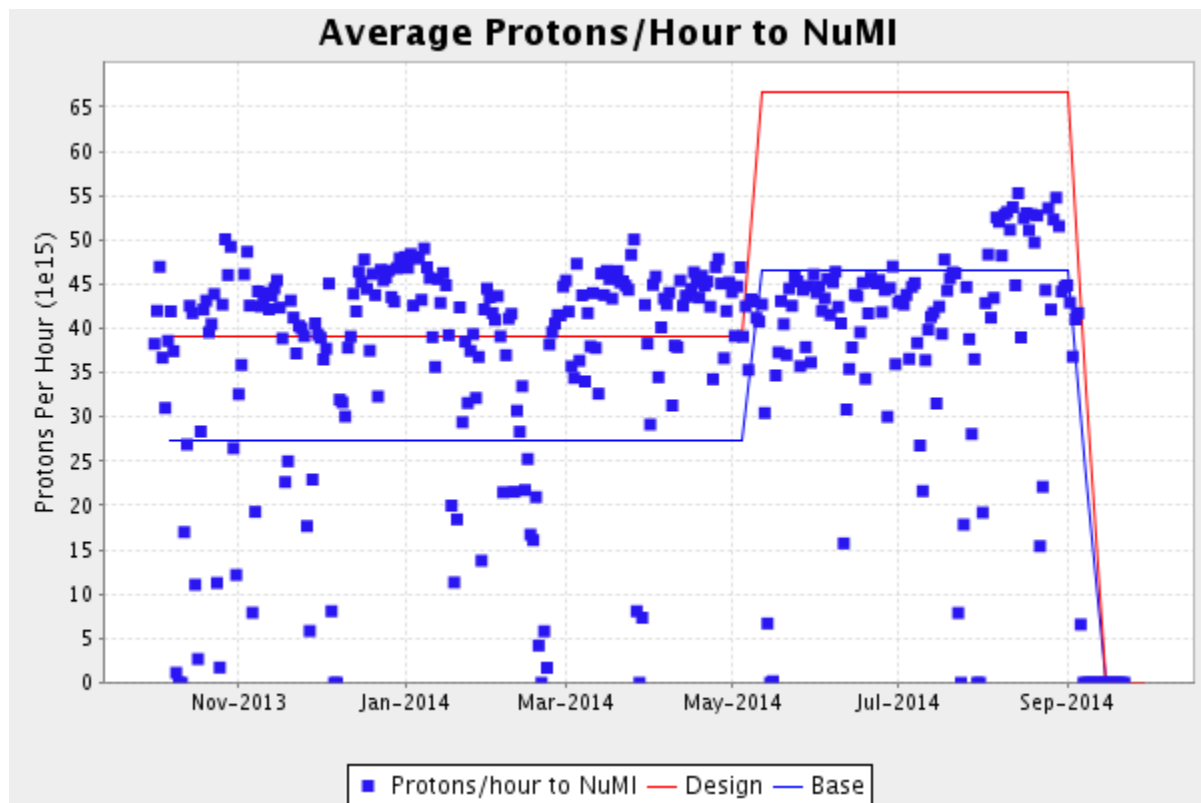
---

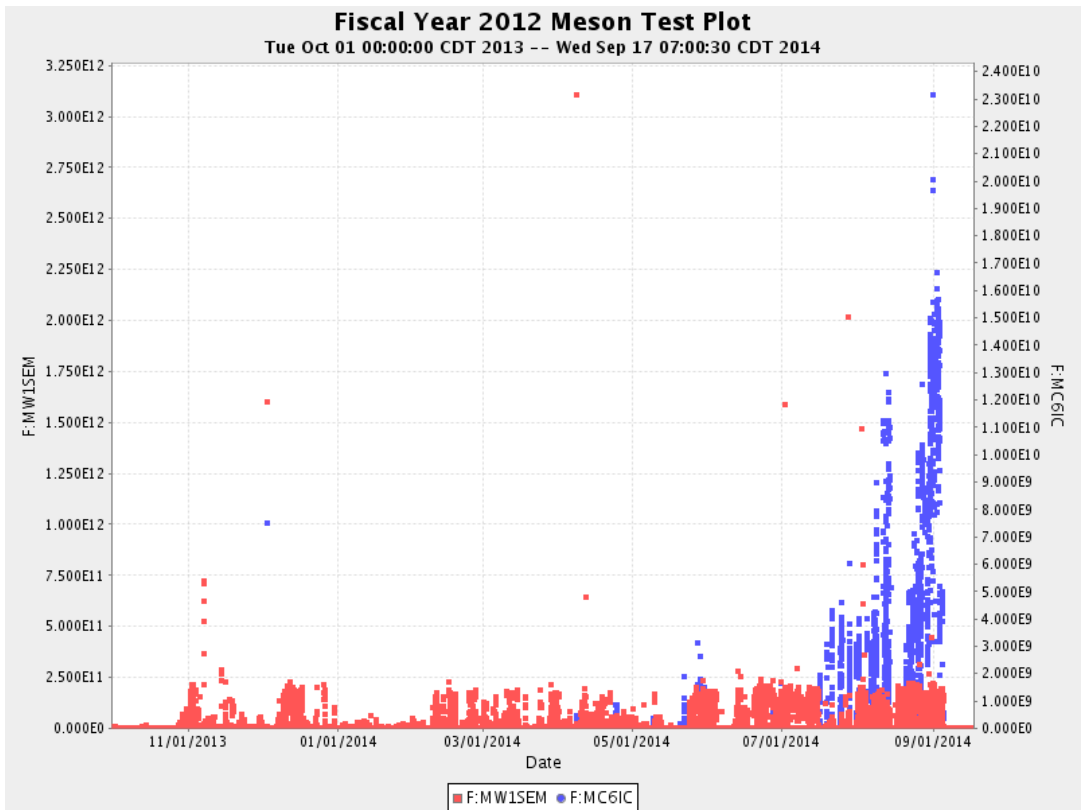
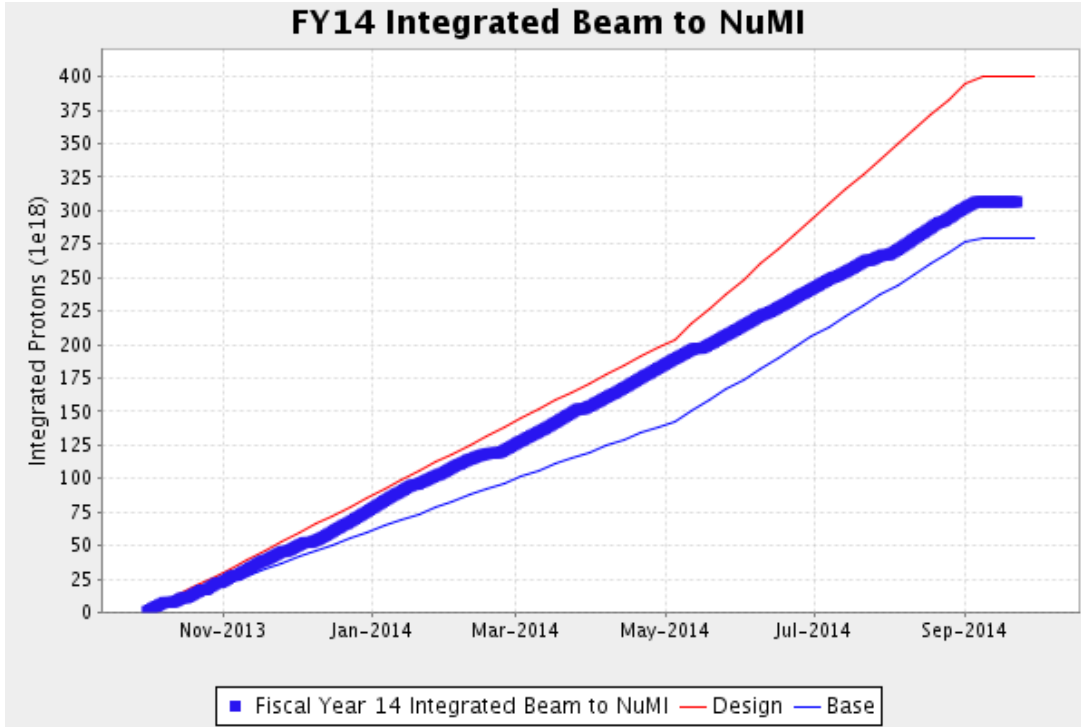
<sup>1</sup> Editor

protons delivered. A great deal of work was required to meet the beam spill structure desired by the experiment.

The Fermilab Test Beam Facility was scheduled for beam for 48 of the 52 week period. Beam delivery started on October 7<sup>th</sup> and continued until September 5<sup>th</sup>. A total of  $7.9 \times 10^{15}$  protons were delivered. The facility operated for 3232 hours driven by user requests and partial shift coverage by the users. One of the additional highlights for the FTBF was the reconfiguration and restart of the Meson Center test beam. This will be supporting a liquid argon detector measurements aimed at future experiments. The MCenter beam operated for 309 hours as requested.

The following plots show the beam delivery over the period.





## MINOS and MINOS+ Progress in FY 2014 (D. Torretta, J. Thomas, R. Plunkett, and K. Lang)

In FY 2014 the MINOS Collaboration continued analyses of data collected in the low energy (LE) NuMI beam setting and was operating the MINOS+ experiment that is continuation of MINOS in the medium energy (ME) beam setting optimized for the NOvA experiment.

The most significant are MINOS results on neutrino mixing that combine all data sets acquired since the beginning of the experiment. This includes the exposure of  $10.71 \times 10^{20}$  protons-on-target (POT) in the neutrino mode,  $3.36 \times 10^{20}$  POT in the antineutrino-mode, and the atmospheric neutrinos exposure of 37.88 kt-y. The analysis of the complete LE data set was performed in distinct steps: first with the two-flavor approximation, then with the three-flavor framework using disappearance data, and finally with the three-flavor framework using disappearance and appearance data. The analysis employs constraints on the value  $\theta_{13}$  from reactor experiments. This is so far a unique approach that produces some of the best constraints on the atmospheric sector of neutrino mixings and oscillations. The results have been recently published in [Phys. Rev. Lett. 112.191801](#), and are shown in Figure M-1 below.

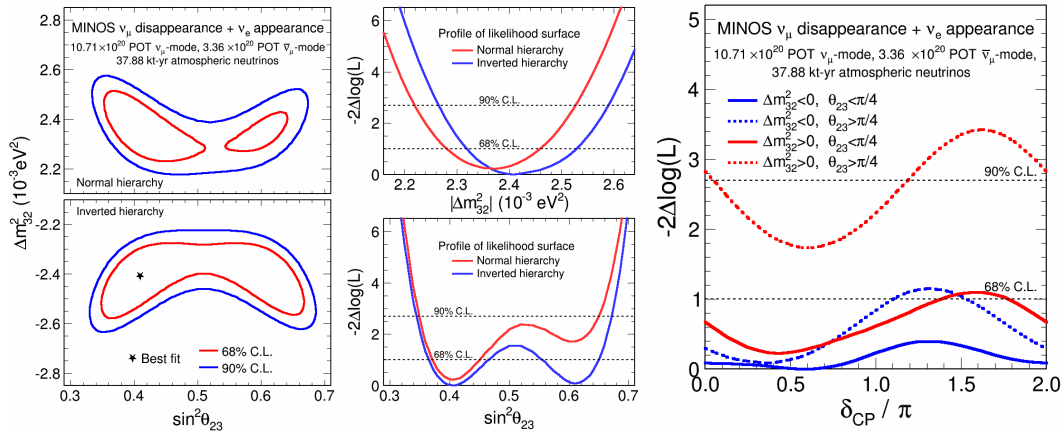


Figure M-1: Results of combined analysis of muon-neutrino disappearance, electron-neutrino appearance and atmospheric neutrinos data. The left panels of this figure show the 2D confidence levels on  $\Delta m^2_{32}$  and  $\theta_{23}$  for the normal and inverted hierarchy. The contours are calculated relative to the overall best fit point of  $\Delta m^2_{32} = -2.41 \times 10^{-3} \text{ eV}^2$  and  $\sin^2 \theta_{23} = 0.41$ , which is indicated by the star. The middle-right panels show the corresponding 1D log-likelihood profiles as a function of  $\Delta m^2_{32}$  and  $\theta_{23}$ . The single-parameter confidence limits are:  $\Delta m^2_{32} = [2.28-2.46] \times 10^{-3} \text{ eV}^2$  (68% C.L.) and  $\sin^2 \theta_{23} = [0.35-0.65]$  (90% C.L.) for the normal hierarchy; and  $\Delta m^2_{32} = [2.32-2.53] \times 10^{-3} \text{ eV}^2$  (68% C.L.) and  $\sin^2 \theta_{23} = [0.34-0.67]$  (90% C.L.) for the inverted hierarchy. This right panels show the 1D likelihood profile for the  $\delta_{CP}$  parameter resulting from the combined analysis of  $\nu_{\mu}$  disappearance and  $\nu_e$  appearance by MINOS using its complete set of accelerator and atmospheric neutrino data. Separate profiles are plotted for each combination of mass hierarchy and  $\theta_{23}$  octant. The best fit occurs in the inverted hierarchy and lower octant; the worst fit is the normal hierarchy and upper octant, which is disfavored by  $-2\Delta \log L = 1.74$ . The dashed horizontal lines indicate the 68% (90%) single-parameter confidence limits, which disfavor 36% (11%) of the three-parameter space defined by the mass hierarchy,  $\theta_{23}$  octant, and  $\delta_{CP}$ .

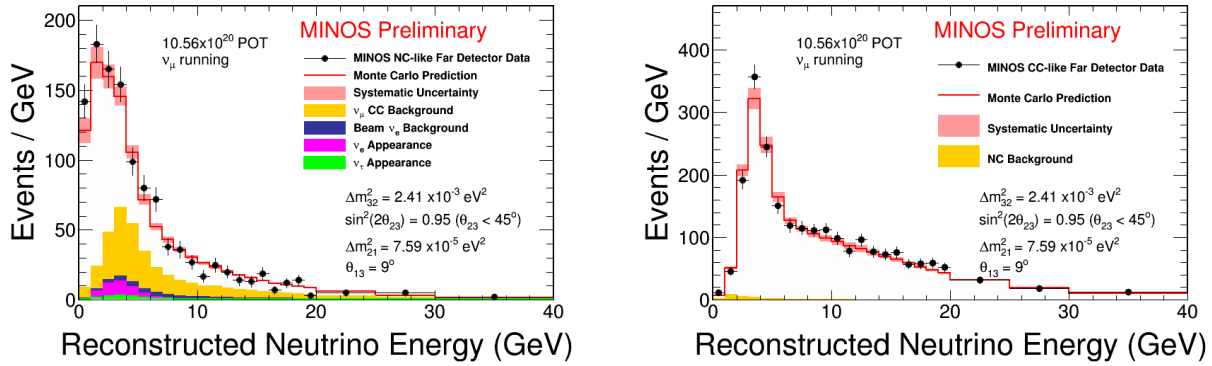


Figure M-2: (Left) This figure shows the far detector prediction of neutral-current reconstructed neutrino energy spectrum including backgrounds and the total systematic uncertainty and compares it to the observed MINOS data. (Right) This figure shows the far detector prediction of charged-current reconstructed neutrino energy spectrum including backgrounds and the total systematic uncertainty and compares it to the observed MINOS data. The prediction assumes a three-flavor oscillation scenario with parameters  $\Delta m_{21}^2 = 7.59 \times 10^{-5} \text{ eV}^2$ ,  $\Delta m_{32}^2 = 2.41 \times 10^{-3} \text{ eV}^2$ ,  $\sin^2 2\theta_{23} = 0.95$  ( $\theta_{23} < 45^\circ$ ),  $\sin^2 \theta_{13} = 0.024$ ,  $\sin^2 \theta_{12} = 0.319$ , and  $\sin^2 \theta_{23} = 0.388$ . No evidence of deviations from the standard three-flavor oscillation picture is found. MINOS uses these results to set limits on the existence of light sterile neutrinos.

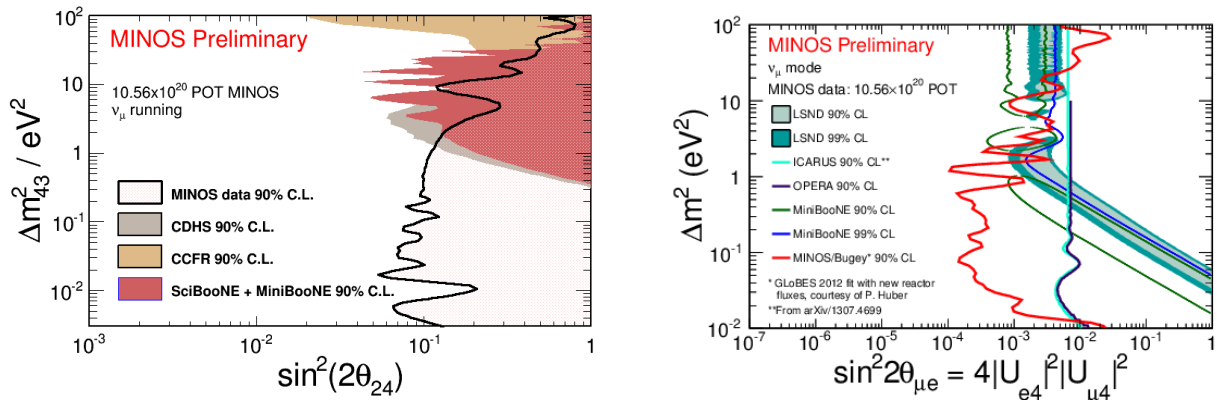


Figure M-3: (Left) MINOS searches for light sterile neutrinos that mix with the active neutrino flavors using charged-current and neutral-current neutrino interactions. No evidence for sterile neutrinos is found in the MINOS data. This figure shows the 90% C.L. excluded regions on the parameter space  $\Delta m_{43}^2$  vs.  $\sin^2(2\theta_{24})$  obtained from the MINOS analysis compared to CDHS, CCFR, SciBooNE and MiniBooNE experiments. MINOS takes advantage of its long baseline and broad energy spectrum to probe previously unexplored regions of this parameter space. (Right) Unitarity constraints generate relationships between  $\nu_\mu \leftrightarrow \nu_e$  transitions and  $\nu_e$  and  $\nu_\mu$  disappearance. In this figure, the  $\nu_\mu$  disappearance results from MINOS are combined with  $\nu_e$  disappearance results from the Bugey reactor experiment to yield 90% C.L. limits on the sterile mixing parameter  $\sin^2 2\theta_{\mu e} = 4|U_{e4}|^2|U_{\mu 4}|^2$  relevant to  $\nu_\mu \leftrightarrow \nu_e$  transition experiments also shown. Regions of parameter space to the right of the red contour are excluded at 90% C.L. The MINOS data correspond to a  $10.56 \times 10^{20}$  POT exposure in neutrino running mode. The Bugey results are obtained from a GLoBES 2012 fit with new reactor fluxes, courtesy of P. Huber. It accounts for the new calculation of reactor fluxes, as described in P. Huber, *Phys. Rev. C* **85** 029901 (2011). The MiniBooNE contours are provided by the MiniBooNE Collaboration and were published in A. A. Aguilar-Arevalo *et al.*, *Phys. Rev. Lett.* **110**, 161801 (2013).

The other results produced over the last year include constraints on sterile neutrinos. By using energy spectra from neutral and charged current events, shown in Figure M-2, MINOS was able to obtain contours that significantly impact the currently available phase space for sterile neutrinos, as shown in Figure M-3 (left). Additionally, by combining the Bugey reactor limits on

the electron disappearance, the analysis constrains the regions accessed by short-baseline appearance experiments shown in Figure M-3 (right).

Since August 2013, MINOS+ has accumulated an exposure of  $3.26 \times 10^{20}$  POT in the ME NuMI configuration out of  $18 \times 10^{20}$  POT requested in the proposal. Before the 2014 shutdown, the beam power was about 320 kW and MINOS+ detectors operated with up-time efficiencies exceeding 95%. The collaboration has been pursuing a suite of analysis activities including detector calibrations and beam simulations – the two fundamental ingredients of deriving physics results. Figure M-4 shows an energy spectrum from the initial part of the FY 2014 run. These spectra are produced using an updated reconstruction algorithm that copes with higher event rate in the ME beam.

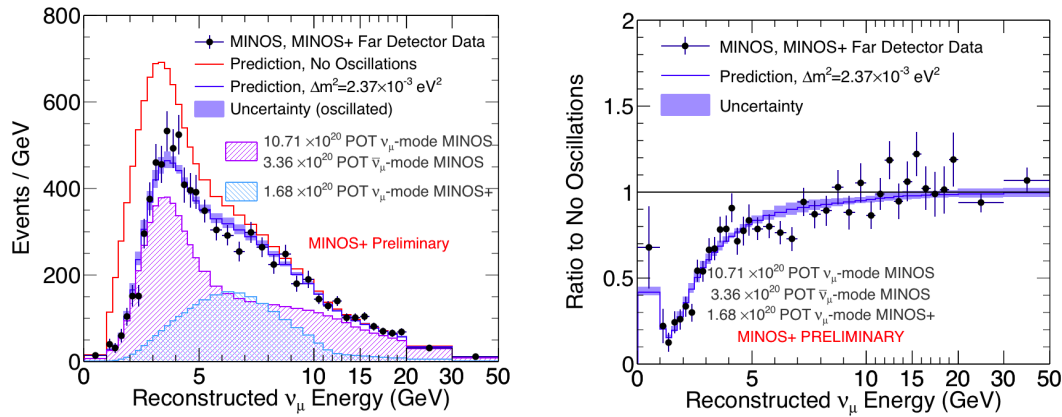


Figure M-4: (Left) The MINOS+ first spectrum of  $\nu_\mu$  and  $\bar{\nu}_\mu$  charged-current interactions in the MINOS+ Far Detector, summed with the existing low-energy data from MINOS. The hatched histograms show the predicted spectra for MINOS and MINOS+, calculated using the best-fit oscillation parameters from MINOS. The two predictions are summed to give a combined spectrum, which is shown by the blue histogram along with its  $1\sigma$  systematic uncertainty band. In addition, the red histogram shows the combined spectrum for the case of no oscillations. The observed data, indicated by the points with errors, are well-described by the oscillation model. The MINOS+ data significantly increase the event yield in the medium-energy region, enabling precision measurements of the  $\nu_\mu$  survival probability curve.

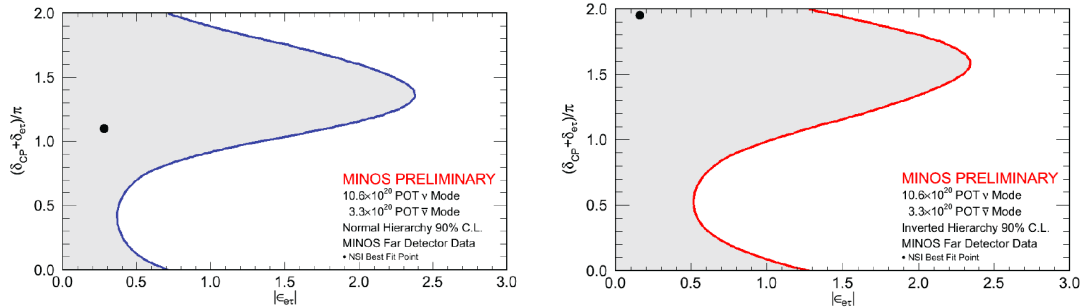


Figure M-5: The appearance of  $\nu_e$  events at the Far Detector is sensitive to the NSI parameters  $\epsilon_{e\tau}$  and  $\delta_{e\tau}$ . These plots show the 90% C.L. allowed values of  $\epsilon_{e\tau}$  and  $\delta_{e\tau} + \delta_{CP}$  assuming a normal hierarchy (left plot) and an inverted hierarchy (right plot). The appearance rate also depends on standard oscillation parameters which are assumed to be the following:  $\sin^2\theta_{23} = 0.5$ ,  $\sin^2\theta_{13} = 0.025$ , and  $\Delta m^2_{32} = 2.43 \times 10^{-3} \text{ eV}^2$ . The contour is produced by marginalizing over the values of  $\delta_{CP}$ .

### ND POT fraction and Live Time Fraction

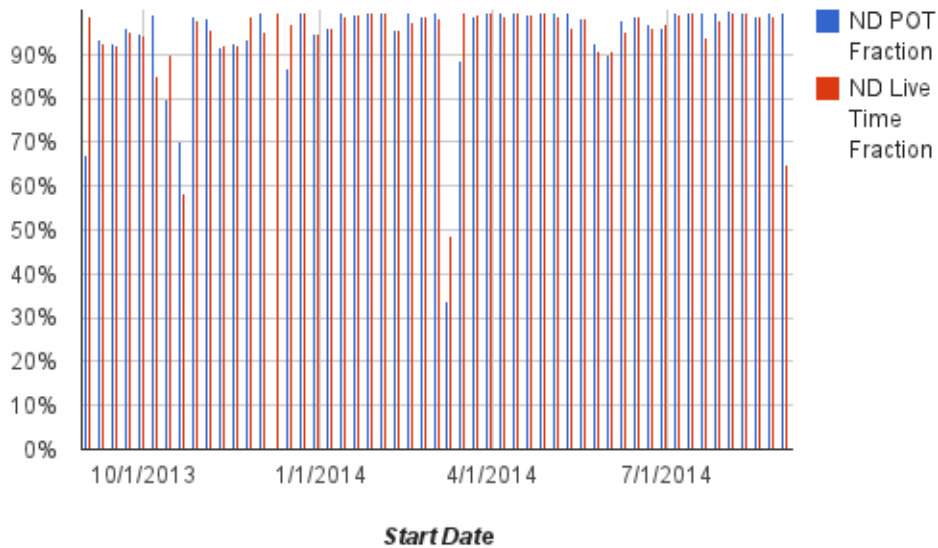


Figure M-6: MINOS near detector live time during FY2014.

### FD POT Fraction and Live Time Fraction

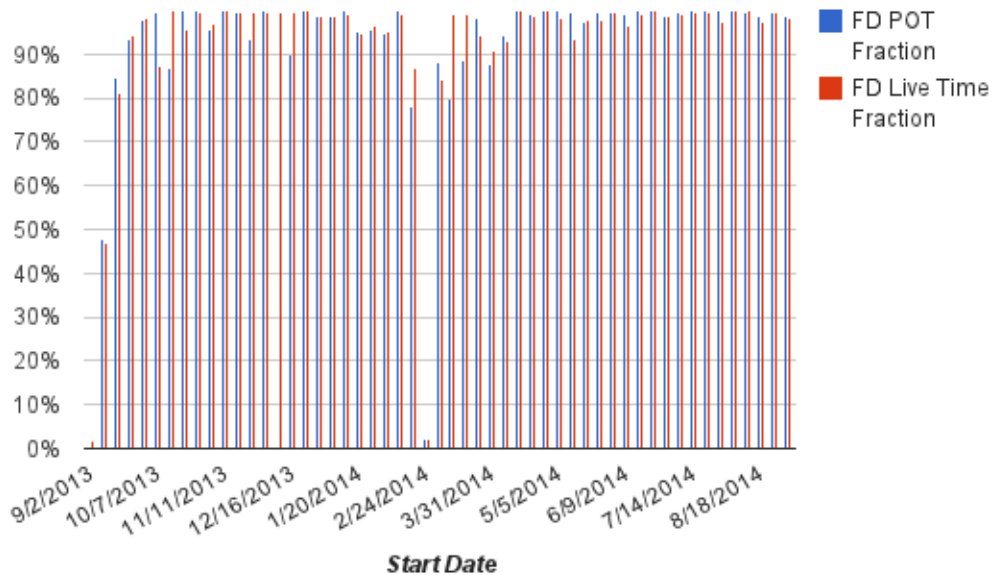


Figure M-7: MINOS far detector live time during FY2014.

While the detector calibration data show routine detector performance, we see beam simulations to be more challenging. The spectrum in the Near Detector is not yet well described by calculations that necessarily include the new target and magnetic horns configuration. Intense work is ongoing in this area.

In parallel, we pursue studies towards the physics program that besides neutrino oscillations includes a search for sterile neutrinos, and more exotic phenomena such as non-standard neutrino interactions (NSI) and large extra dimensions (LED). Figure M-5 shows the sensitivity to some

of the NSI parameters available through the analysis of MINOS data. We plan to open some analysis boxes in the not-too-distant future and announce the first MINOS+ results on neutrino oscillations.

The MINOS+ Collaboration is looking forward to running with upgraded intensity through the Proton Improvement Plan that would enable the proposed physics program of the experiment.

MINOS+ operations in FY 2014 were smooth and highly automated, which is reflected in live times consistently greater than 95% and often as high as 99%, at both near and far detectors (figures M-6 and M-7 show the live time for each of the detectors).

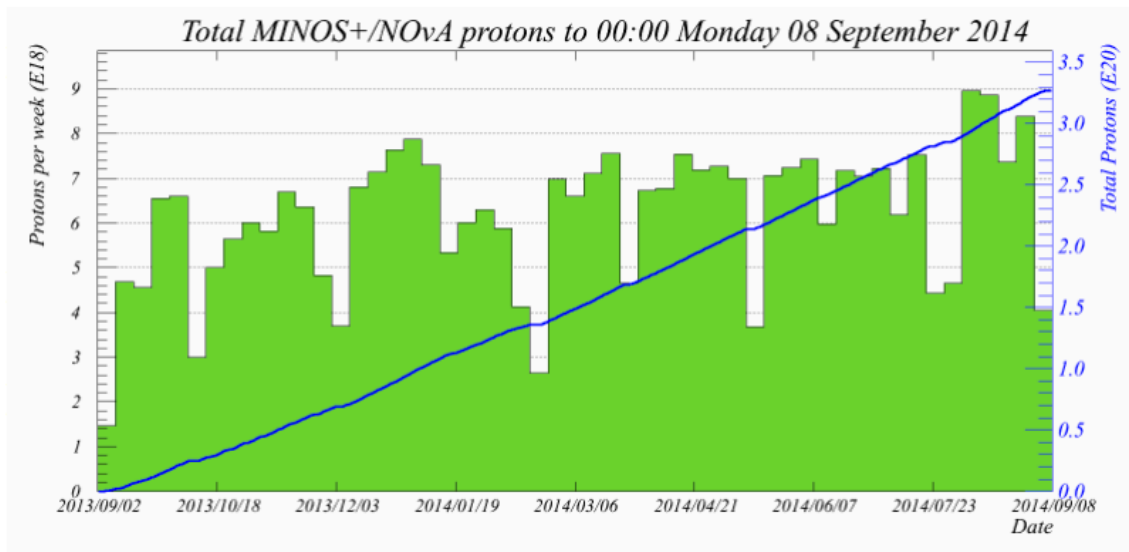


Figure M-8: MINOS+ NuMI beam delivered to MINOS+ during FY2014.

During this period, MINOS+ collected  $3.26 \times 10^{20}$  POT, as shown in figure M-8.

The new Ethernet based DAQ installed in 2013 at the Near Detector performed very well during this period, while the original PVIC based DAQ still in use at FD caused several downtimes. An unexpected serious hardware failure of the FD DAQ in March 2014 forced an immediate conversion of the FD DAQ to the new Ethernet based DAQ. The new DAQ was operational in a few days of hard work and has been stable since. In May 2014 DAQ dependencies on the NFS BlueArc storage system were removed, eliminating a downtime due to its regular maintenance and own failures. Tests have been performed to show that the experiment can run disconnected from the Network, if necessary. Data can be written on local disks and copied to final storage and production machines by temporarily enabling the network connection. At the near site, the experiment installed a new sealed DAQ rack with dedicated AC unit, for long-term protection of the equipment from dust and dirt. The new rack passed necessary reviews in September 2014 and all DAQ computers and gateways have already been moved into the new rack.

During the shutdown, which began in September 2014, MINOS+ is commissioning new timing readout computers at both FD and ND, to replace the old (2000-2001) computers, which are obsolete. The timing electronics will remain unchanged. Investigations are underway concerning

cleaning of the electronics boards at the near detector to prevent future possible maintenance during runs due to dust accumulation.

### E-944 / MiniBooNE (R. Tayloe, R. Van de Water)

For FY 2014 the Booster Neutrino Beamline (BNB) and the MiniBooNE detector ran in beam-dump mode to enhance the search for light dark matter. During this time the beam-line and detector ran stably, and beam delivery from the Booster was excellent, with a total of  $1.88 \times 10^{20}$  POT. Shown in Figure MB-1 is the POT delivery rate and neutrinos/POT, which demonstrates the overall experiment stability through the run. The beam-dump data are currently being analyzed and results should be coming out in FY2015.

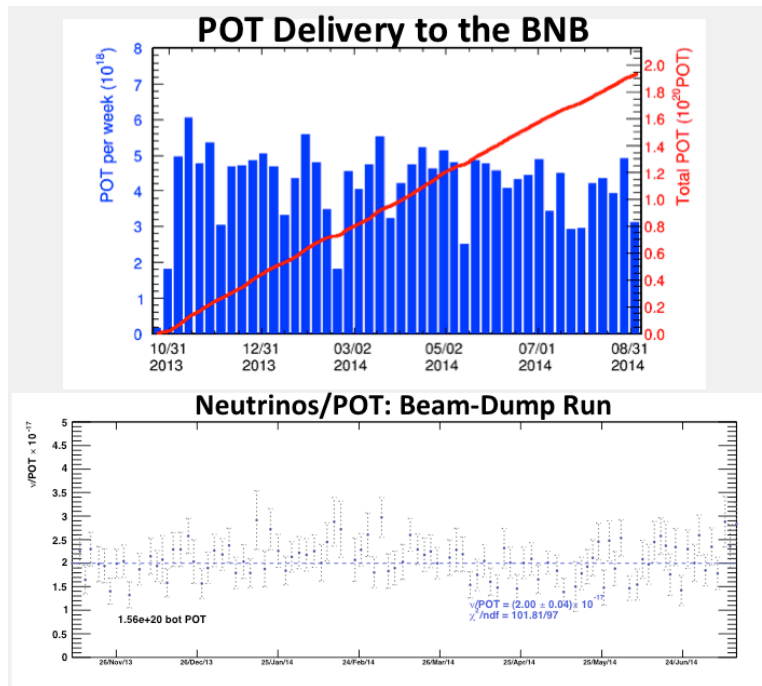


Figure MB-1: The top plot shows the POT delivery to the BNB during FY2014 in beam-dump run configuration. The bottom plot shows the reconstructed neutrinos per POT during the run, demonstrating stability of the beam-line and detector during the run.

All these recent results are interesting and continue to motivate and guide experimental and theoretical work on neutrino and antineutrino cross-sections and short baseline oscillation.

The beam-dump mode configuration is shown in Figure MB-2. Here the proton beam is steered passed the target through a 1 cm air gap between the target and horn. The protons then travel 50 m through the decay pipe and impact the absorber at the end of the pipe. Most secondary mesons produced by the proton interactions in the Fe-absorber are absorbed before they can decay, significantly reducing the neutrino rate in beam dump mode relative to neutrino mode. Using the reconstructed CCQE muon neutrinos, the measured rate between neutrino mode and beam-dump mode is  $\text{Rate}_{\text{CCQE}}(\text{Neutrino}/\text{BeamDump}) = 48 \pm 2$ . Figure MB-3 shows the measured beam-dump mode CCQE muon neutrino reconstructed energy compared to the Monte

Carlo beam-dump predictions. The energy of the two distributions agrees well, although the beam-dump rate is scaled up by a factor of 1.6. We are investigating the source of the increased neutrino rate and looking at the possibility of extra materials (beam pipe window, horn window, etc.) that are missing from the Monte Carlo. In neutrino mode these missing materials would have a sub-percent effect, but because of the reduce neutrino flux in beam-dump mode, have significant contributions. The dark matter analysis background predictions are tied to the observed CCQE muon rate, which are the source of these backgrounds, and so the extra flux is properly accounted for in the search analysis.

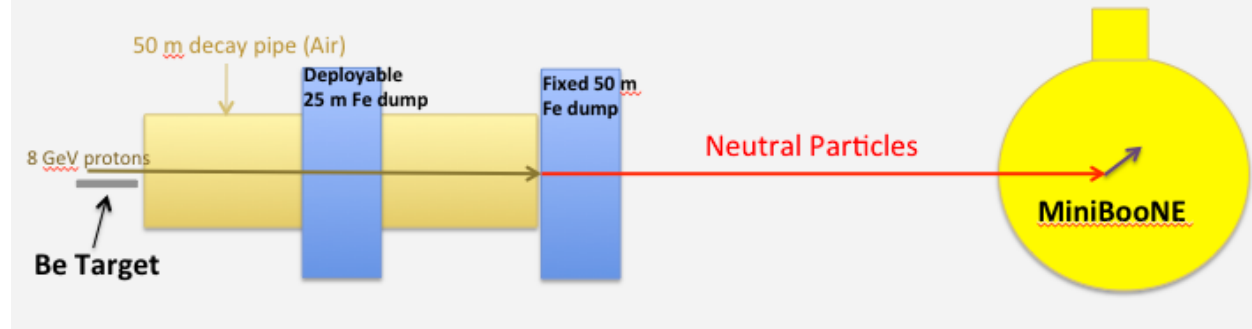


Figure MB2: BNB beam-dump run configuration. The protons are steered past the Be target and horn, travel the length of the decay pipe and interact in the 50 m Fe-absorber. Neutrino production is reduced by a factor of 48 relative to neutrino mode. Most neutrinos produced in beam-dump mode come from proton-air interactions in the decay pipe.

The BNB itself received two upgrades to improve the beam line monitoring and physics reach of the experiment during the beam-dump run. Two new low mass multiwire chambers were installed just upstream from the target/horn. The multiwire chambers are separated from each other by 1m, and can remain in place during beam running. This allows for improved positioning of the proton beam on the target. It also significantly improves the beam angle determination, which is required to reconstruct the projected proton beam spot position in the MiniBooNE and MicroBooNE detectors. Figure MB-4 shows a schematic of the multiwire chambers, and the proton profiles from a typical event. The pointing resolution achieved, on an event-by-event basis, is 0.25 milli-radians. This translates into a projection at the MiniBooNE detector of 13 cm. Knowing the location of the projected proton beam spot is important for exotic physics searches such as low mass dark matter, axions, paraphotons, etc.

Another upgrade is the high rate digitization of the Resistive Wall Monitor (RWM) timing waveform, and the installation of a new high-speed discriminator and fiber optic transmission line from MI12 to the MiniBooNE detector hall. Figure MB-5 shows a plot of the reconstructed CCQE muon timing relative to the beam RF bunch structure. All 81 bunches are overlaid onto one. The muon timing resolution is better than 2 nsec. Events  $\sim 4$  nsec beyond the mean are out of time with the beam RF and are most likely dirt or cosmic backgrounds. Due to MiniBooNE's excellent veto and reconstruction techniques, not much background resides in the tails of the muon timing sample. However, other samples such as electrons, and at low energy, benefit from this extra information to identify backgrounds. These upgrades significantly improve the measurement of the time of flight of particles from the target to the detector, which allows for a search of  $>50$  MeV long-lived particles being produced by proton interactions in the target, and helps identify and characterize dirt and cosmic backgrounds that reside out of time with the beam

RF structure. This will be important for background suppression in LAr detectors running on the surface.

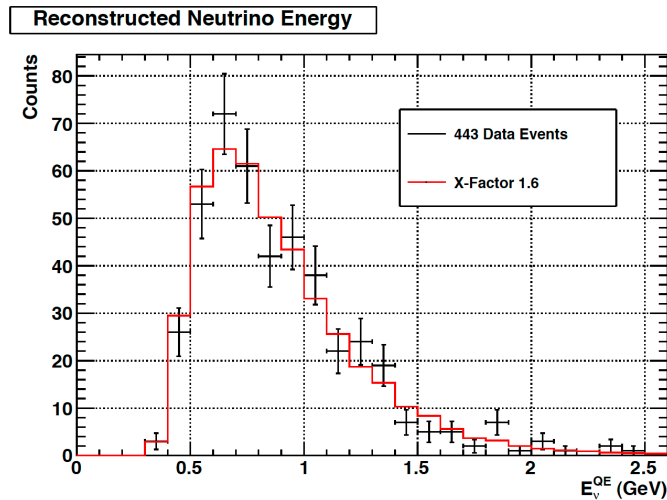


Figure MB-3: The MiniBooNE beam-dump mode reconstructed neutrino energy for data (error bars) and beam-dump Monte Carlo (red line). The MC was scaled by a factor of 1.6 to match the data. The source of the difference is currently being investigated.

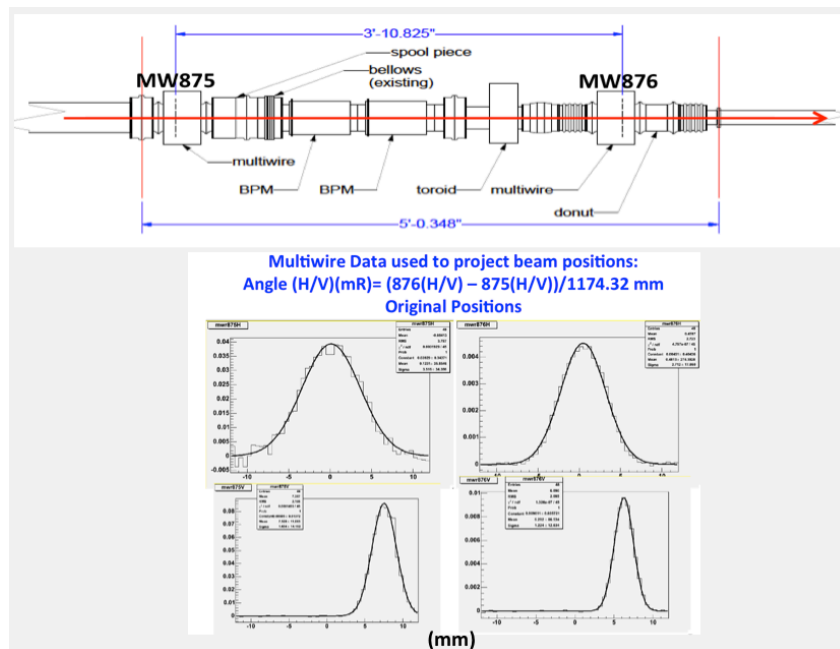


Figure MB-4: Top figure shows the new dual multiwire chambers installed at the 875/876 positions in the BNB. The bottom figure shows the Horizontal (top) and Vertical (bottom) proton beam profiles for both MW875 (left) and MW876 (right). Using both multiwire chambers allow a beam projection resolution of around 0.25 milli-radians for each spill.

Both of these key BNB upgrades are important to the future SBN program and will be utilized by MicroBooNE, LAr1-ND, etc., to enhance and extend their physics reach. The potential of these devices for LAr detectors are just starting to be investigated, and appreciated.

An important aspect of continued running of the BNB for MicroBooNE and LAr1-ND is the reliability of the beamline and horn. During the FY 2014 beam-dump run period, the combined BNB beamline and detector uptime was over 95%. The most crucial element, the horn and target, did not operate during this time since we were in beam-dump mode. However, we continued to run the horn RAW systems, monitored water and radioactivity activity levels, temperatures, etc, to ensure the beam-line was operating properly. The current horn/target has over 390 million pulses, surpassing the first horn which failed eight years ago with 94 million pulses. Both these numbers were world records at their respective times. In the unfortunate event of complete failure, a spare horn and target are available. It would require four to six weeks to install the replacement system. As well, the pieces for a fourth target and horn (horn #1 is dead, horn #2 is operating, horn #3 is the immediate spare) are being assembled and will be available by FY2015 should the need arise.

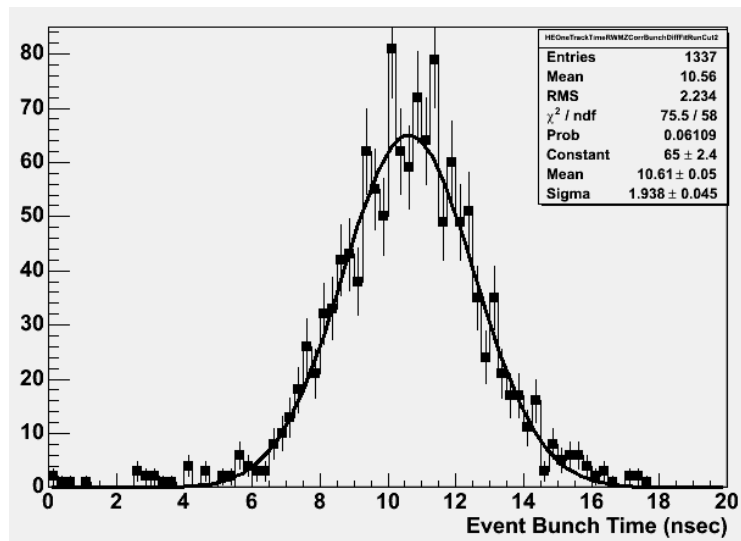


Figure MB-5: Shown is the beam-dump CCQE muon reconstruction bunch time (relative to the beam RF structure) using the new timing system. The system resolution is  $\sim 2$  nsec, and stable over long run periods, allowing its use as an important variable in the physics analysis.

### **E-938 / MINERvA** (D. Harris, K. McFarland)

#### *MINERvA Construction and Installation Activities in FY 2014*

The MINERvA experiment began taking physics quality data in November 2009 while the last components were being built and commissioned. By mid-March 2010 the installation was completed and the experiment started taking data with the full active detector, and all of the solid targets installed. By the beginning of FY 2012 the cryogenic target was filled with Helium, and the veto wall upstream of that target was fully commissioned and operational. In FY 2011 the experiment added a water target. The experiment took data throughout FY 2012 in the NuMI Low Energy beam. During the FY13 shutdown the MINERvA experiment upgraded its Data Acquisition system and upgraded the roof over the detector to protect it from water damage. In FY14 the MINERvA experiment took data in the NuMI Medium Energy beam. One additional site qualified to take remote shifts during FY14: University of Minnesota-Duluth. During FY14

run the experiment ran approximately 40% of its shifts remotely.

Over the course of FY14 MINERvA collaborators together with PPD's EED group upgraded the data acquisition firmware so that the experiment would have improved diagnostics in case of electronics failures. In addition the DAQ firmware was changed to allow more events to be stored within one beam spill. This increased capability will become important as the protons per pulse increases, which is expected to happen over FY15. This new capability will also be important for the medium energy test beam run. A new spare Light Injection Box to be used on the neutrino detector was also commissioned and built at the University of Pittsburgh over most of FY14.

The MINERvA collaboration also started preparations for the medium energy test beam run, which is to start in FY15 after the accelerator shutdown is over. In addition to improving the DAQ firmware, in FY14 MINERvA also purchased 13 new multi-anode phototubes that were subsequently placed in special housings that protect the tubes from magnetic fields and also support the PMT bases and front-end electronics. Significant work was done at SciDet to help MINERvA diagnose problems with (older) PMT alignment that was leading to high crosstalk values between neighboring pixels. New fixtures were produced and by the end of FY14 the experiment has enough PMT's installed in housings and tested to support a simultaneous medium energy test beam run (41 tubes), detector operations (507 tubes) and a small spare tube stock (5 tubes). Once the test beam run is over (estimated at February 2015) the spare stock will be at a more reasonable level given a possible run time of an additional 4 years.

#### *Physics Goals for MINERvA in Low Energy Beam*

The goal during the low-energy neutrino running was to provide exclusive cross-section measurements on a variety of nuclei. The data will help in understanding the details of neutrino interactions. Low energy events tend to have few final state particles – which allows the MINERvA detector to identify single particles and the exclusive channels important for current and future oscillation experiments. MINERvA's detector is about a factor of 10 more fine-grained than the NOvA detector, and can identify processes that will contribute backgrounds to NOvA. MINERvA sees a higher neutrino beam energy than T2K's near detector, and measures reactions that contribute backgrounds to T2K from the high-energy tail of the beam (where “high energy” in the T2K case means above 1 GeV).

MINERvA achieved the first of its physics goals in FY13 by publishing a high statistics measurement of the quasi-elastic neutrino interaction, for both neutrinos and antineutrinos (Physical Review Letters (2013, volume 111, 022501, and 00022502). In the beginning of FY14 MINERvA reached another milestone when it released its measurements of cross section ratios between iron and scintillator, and lead and scintillator. These results, shown in Figure MV-1 are the first direct measurement of nuclear effects in neutrino scattering and disagree with the predictions that are based on nuclear effects as measured in charged lepton scattering (Physical Review Letters (2014, volume 112, 231801).

MINERvA also produced results in FY14 on the scintillator target, which is primarily hydrocarbon. A measurement of the cross section for inclusive pion production in charged current neutrino interactions was submitted for publication in June 2014 [arXiv:1406.6415]. This is an important process that must be understood, because it not only provides a substantial fraction of signal events for NOvA, but also because it represents a background for quasi-elastic

events in T2K and other water Cerenkov detectors. This cross section on deuterium is not well known, and in addition the nuclear effects, expected to be substantial, have not been seen at the expected strength in the MiniBooNE measurement of this process (Phys. Rev. D 83, 052007 (2011)). MINERvA's low pion energy threshold and good tracking resolution allows a precise measurement of the pion kinematics for this process, and clearly shows the effects of final state interactions on the outgoing pion (shown in figure MV-2 on the right).

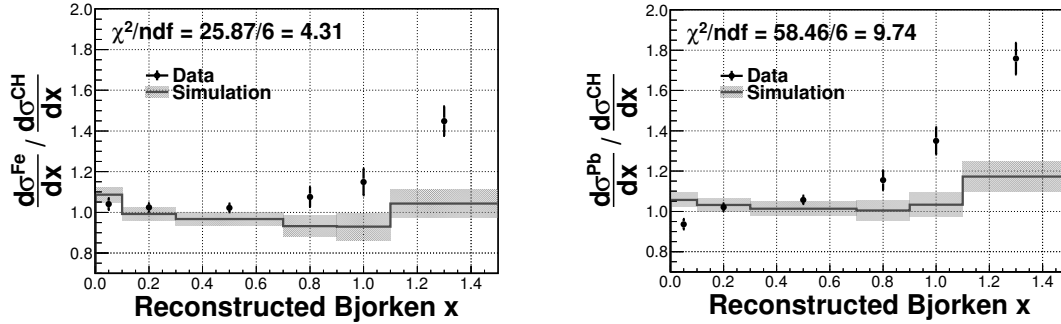


Figure MV-1: MINERvA's measurements of cross-section ratios between iron and hydrocarbon (left) and lead and hydrocarbon (right) as a function of the fractional momentum of the struck quark in the parton model ( $x_{\text{Bjorken}}$ ). From Physical Review Letters (2014, volume 112, 231801).

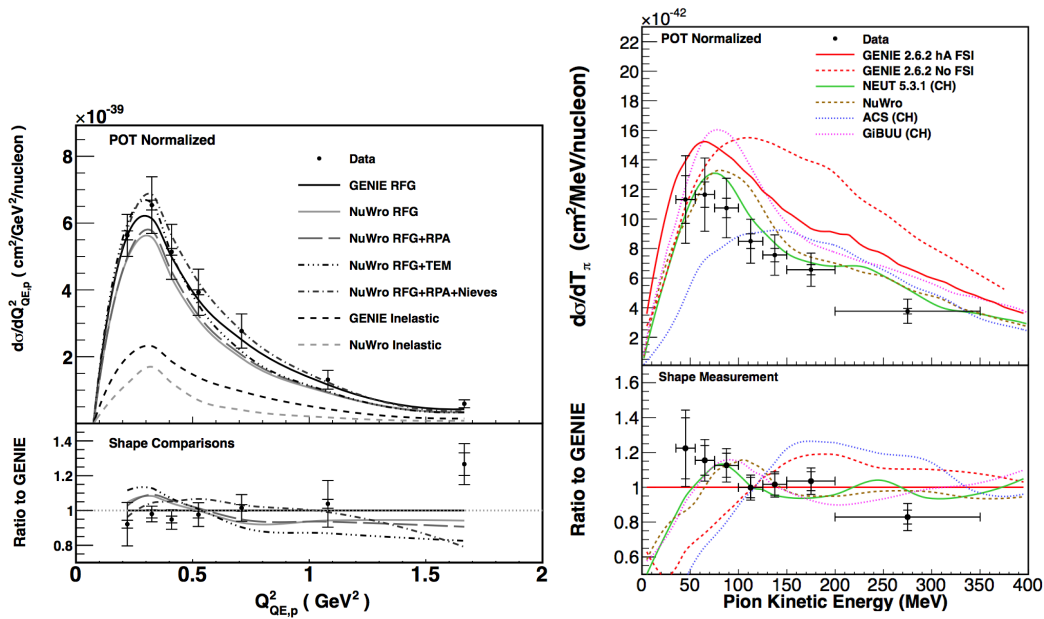


Figure MV-2: (left) shows the cross section for quasi-elastic like events as a function of the four-momentum transfer squared as measured by the proton kinematics. (Right) shows the cross section for neutrino charged current pion production as a function of the pion kinetic energy. In both cases the smaller error bars are the statistical errors, and the larger error bars are statistics plus systematics. In the lower plots the ratio of the data and several models to the default (GENIE) prediction is shown, where each prediction is normalized to the data.

MINERvA released a measurement of the neutrino quasi-elastic interaction on hydrocarbon as viewed from the kinematics of the outgoing proton rather than the outgoing muon (shown in figure MV-2 on the left) [arXiv:1409.4497] in FY14. The energy imparted to the proton in that

interaction is an important input into models that are used to reconstruct neutrino energies. Since this process is a dominant signal channel in oscillation experiments, this measurement has significant impact on future precision oscillation measurements. The MINERvA result shows that the models that best describe the leptonic side of this process are not the same as the models that best describe the proton side of the process. New models can use these as a new and unique constraint on the hadronic process and the final state interactions of the proton.

Finally, at the end of September 2014 a new measurement of charged current coherent pion production in both neutrino and antineutrino interactions, was submitted for publication [arXiv:1409.3835]. This is a process where the neutrino imparts no momentum to the nucleus but produces a pion coherently off the entire nucleus. Coherent scattering has been seen at higher neutrino energies but specifically not seen around energies of 1 GeV. The neutral current analog of this process is rare but poorly constrained and therefore important background to oscillation experiments because there is only one very forward-going neutral pion in the final state. The MINERvA measurements are unique because they can isolate the reaction in a model-independent way, and then test the final kinematics against the models. The data show an even more forward spectrum of the pion angles than is predicted by the models, which would imply higher backgrounds in the neutral current analog for oscillation experiments.

#### *Time Line of MINERvA Operations*

MINERvA started taking antineutrino physics-quality data with its partially completed detector in November 2009. For this detector, the entire downstream hadron and electromagnetic calorimeters were installed, as well as about half the active target modules. After January the remaining 45% of the detector was installed. During the second installation period, from January 2010 through March 2010, the downstream detector components remained in a stable configuration and the experiment continued to take antineutrino data. During this period of time the Argoneut detector was situated between the MINERvA and MINOS detectors, making energy reconstruction for muons passing between the two detectors very difficult to model accurately enough for a precision cross section experiment. As a result, the data taken during this period could not be used for MINERvA's first physics publication, but was used for the first time in a publication in the antineutrino coherent scattering result that was produced this year.

On March 22, 2010 the detector installation and checkout was completed and the neutrino running began. This run includes all of the solid nuclear targets that are planned for the experiment. The live times quickly reached the 95% level and above after about a week of running, and have been stable and high since that time. Over the entire Low Energy run (March 22, 2010 through April 26, 2012) the integrated live time of MINERvA was 97.1%, and the experiment integrated  $3.04 \times 10^{20}$  POT when both MINERvA and MINOS Near Detectors were collecting data.

The data taken in FY 2014 was all Medium Energy neutrino data. There were two special runs taking during this time: one where the protons per pulse was reduced to only a tenth of the nominal to study rate-dependent effects, and one period where the horns were not pulsed to measure the high energy tail of the neutrino flux without the focusing peak. Between October 1, 2013 and September 30, 2014, the experiment received  $3.08 \times 10^{20}$  POT over all running modes. The MINERvA detector was live for 97.5% of the protons delivered on target. The cryogenic helium target was filled in January 2014 after the experiment had integrated roughly  $0.6 \times 10^{19}$  POT with no helium (to be used for background subtraction in the helium analyses). During this

running period the experiment was able to calibrate the detector, monitor the detector light levels, and check the reconstruction performance of both the MINERvA and MINOS detectors continuously, and much more quickly after the data were taken than in the Low Energy run.

**Fixed - Target Switchyard 120 GeV (SY120) and MTest** (A. K. Soha, C. D. Moore, P. Reimer)

The general operation of SY120 was relatively smooth. The major upgrade was the installation and commissioning of the MCenter Beamline with a final tertiary beam capability for the LArIAT experiment. The beam losses for Meson and SeaQuest were manageable; however during the present shutdown (Fall 2014) improvements to the aperture in the G1 stub area of SY120 will enable increased beam intensity to SeaQuest if the duty factor continues to permit increased intensity per pulse. Also during the shutdown work on improving the cathodic protection system will continue.

### **E906/SeaQuestDrell-Yan:**

The SeaQuest experiment (E906) is measuring the ratio of the d-antiquarks to u-antiquarks in the proton and the nuclear dependence of antiquark distributions in the x range of 0.1-0.5 using the Drell-Yan reaction in di-muon production. Additional measurements from the same data set will include the energy loss of fast quarks in cold nuclear matter and the nuclear dependence of J/ $\psi$  production. The experiment had a commissioning run in March-April 2012 that allowed for testing of the spectrometer as well as the beam line and proton slow spill extraction from the Fermilab Main Injector. Following the fifteen month accelerator shutdown and a second repair of our beam line vacuum, the experiment started receiving 120 GeV beam in November 2013 and began taking physics data in March 2014.

As of September 2014, production data has been accumulated with  $2.7 \times 10^{17}$  live protons (approx. 5% of the experiment's goal) on targets of hydrogen and deuterium for the dbar/ubar measurements (70% of beam protons) and carbon, calcium and tungsten for studies of nuclear dependences and to place limits on the nuclear correction for deuterium (30% of beam protons.) The performance of the apparatus is well described by the Monte Carlo simulations demonstrating that the experiment has the expected acceptable mass and other kinematic resolutions and good target to dump separation. (See Figure SQ-1.)

During the shutdown in FY13 SeaQuest completed several upgrades to the spectrometer. A new tracking chamber was constructed and installed to replace the Station 3 tracker that had been recycled from the previous Drell-Yan experiments (E866, E789, E772 and E605). The bases of the photomultipliers on the trigger hodoscopes were modified to better handle high rates. In addition, upgrades to the DAQ (TDC zero suppression) and computing cluster (more data storage and computing capability) were implemented. Additional beam monitoring capabilities were added, including a beam-line Cherenkov counter that is able to measure beam intensity variations on the 53 MHz scale to diagnose beam spill problems and inhibit data taking during rf buckets with abnormally high intensity. A parametric current transformer monitor will be installed in September 2014 to measure the absolute beam intensity to 1%.

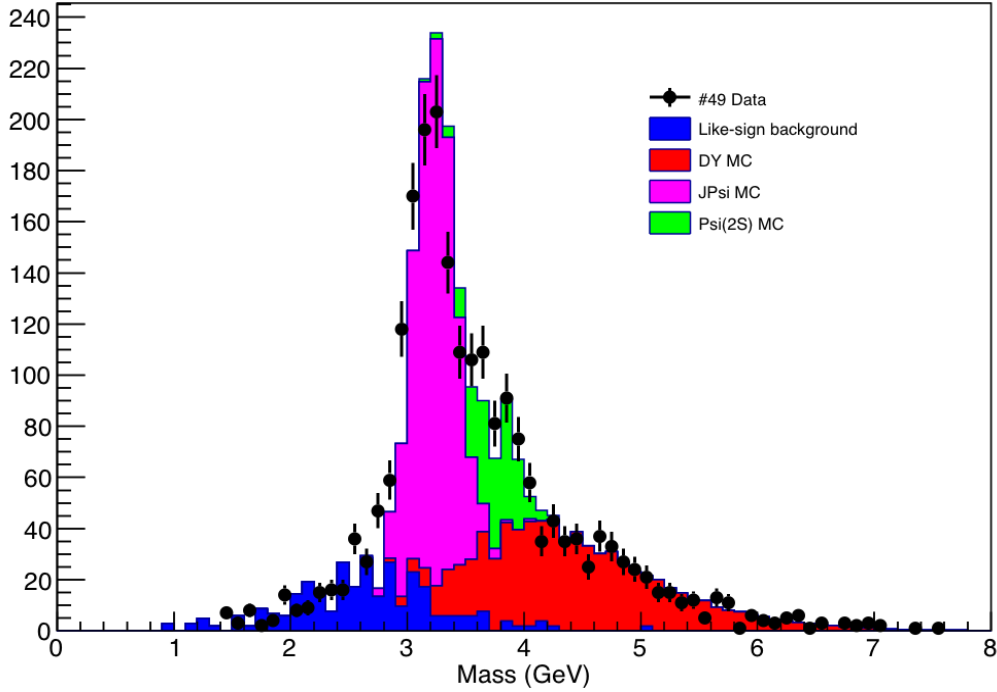


Figure SQ-1: Reconstructed mass distribution of di-muon events from a few days of data compared to Monte-Carlo simulations.

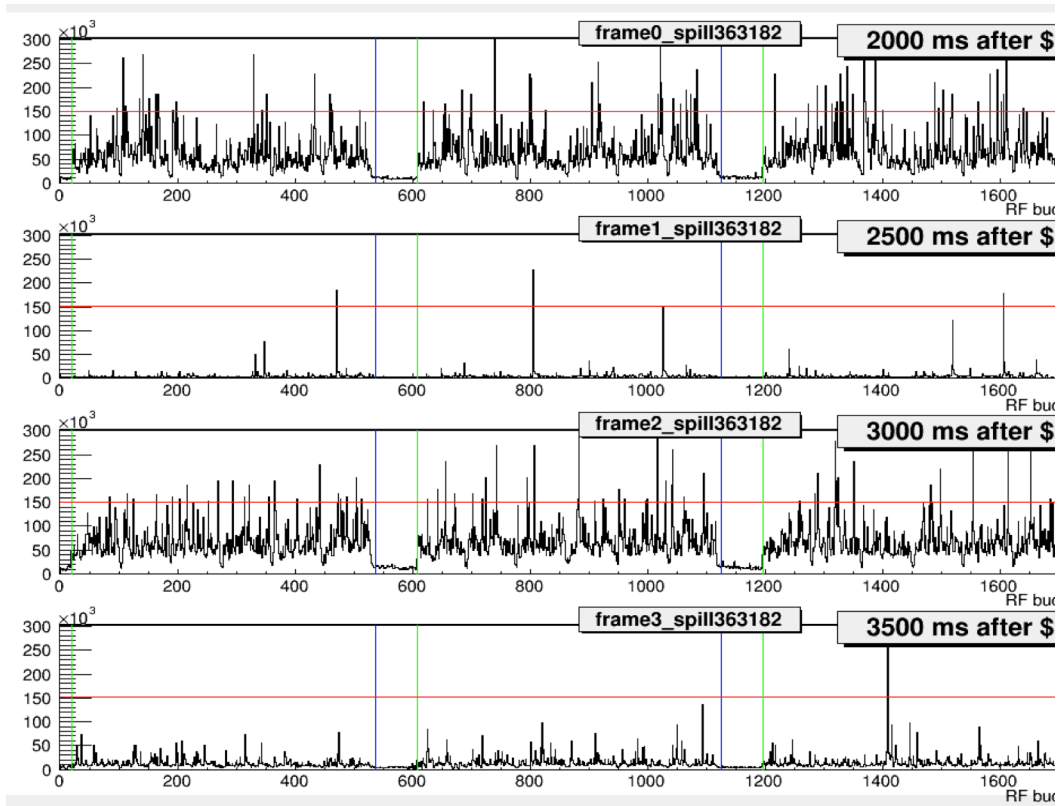


Figure SQ-2: Beam intensity per rf bucket for the extraction of twelve turns of the main Injector: three turns at 2000 ms (top), 2500 ms (middle-top), 3000 ms (middle-bottom) and 3500 ms (bottom) after the start of spill. For any bucket above the red line, the trigger is inhibited for 10 buckets centered on this bucket.

The extracted beam continued to have poorer-than-desired duty factor so running started at 1/10th nominal intensity. The duty factor is monitored by three independent techniques: 1) a direct measure of the beam, rf bucket by rf bucket, by the beam Cherenkov counter, 2) the relative rates of random coincidences and individual hits between widely separated scintillators, and 3) the number of counts in a scintillator read out every 133  $\mu$ s. The first two give consistent measures of the duty factor at 53 MHz. The last measures the duty factor at 7.5 kHz and typically gives average duty factors per spill that are 2-2.5 times higher; because it averages over about 7,000 rf pulses. The beam Cherenkov counter is used to veto for a period of 190 ns around beam buckets that have greater than ten times the average intensity (See Figure SQ-1). As the Accelerator Division learned to improve the duty factor (to about 25-30%), the intensity was increased to  $4\text{-}6 \times 10^{12}$  protons per pulse (the intensity requested in the proposal was  $1 \times 10^{13}$  ppp) but about 40% of this beam is vetoed due to high individual bucket intensities. The high intensity buckets lead to unacceptable random trigger rates as well as significant additional track noise in the spectrometer that together have a strong impact on readout dead time, number of events that must be reconstructed and overall reconstruction efficiency.

During the two-month shutdown in September and October 2014, the experiment will install a new tracking chamber to replace the temporary Station 1 chamber. The new chamber will have better rate capabilities, allowing for higher luminosity and the wider acceptance needed to improve the efficiency for high- $x_{\text{Target}}$  events. Production analysis of the FY14 data set is now being done on the Fermilab Grid computing systems and the first pass should be completed by Oct 2014.

The experiment currently has twelve graduate students whose Ph.D. thesis data will be collected in E-906/SeaQuest. There are also eleven undergraduate students and seven postdoctoral research associates working on the experiment. Recent studies have shown that the apparatus, as a classic beam stop experiment, also has sensitivity to dark photons (sought as a possible form of dark matter) in a unique regime of mass and coupling constant. This physics is also being pursued.

### *The Fermilab Test Beam Facility*

The Fermilab Test Beam Facility (FTBF) gives users from around the world an opportunity to set up their particle detectors in a variety of particle-beams. A plan view of the facility is shown in Fig. TB-1. The web-site URL for the facility is [www-ppd.fnal.gov/FTBF](http://www-ppd.fnal.gov/FTBF). Since it began operation in 2005 the facility has served 58 experiments, consisting of 835 individual experimenters from 177 institutions, in 30 countries.

### *Research Performed at the FTBF in FY 2014*

Each test-beam experiment is required to prepare a Technical Scope of Work (TSW) with the Laboratory, in which the beam, infrastructure, and safety requirements are spelled out in detail.

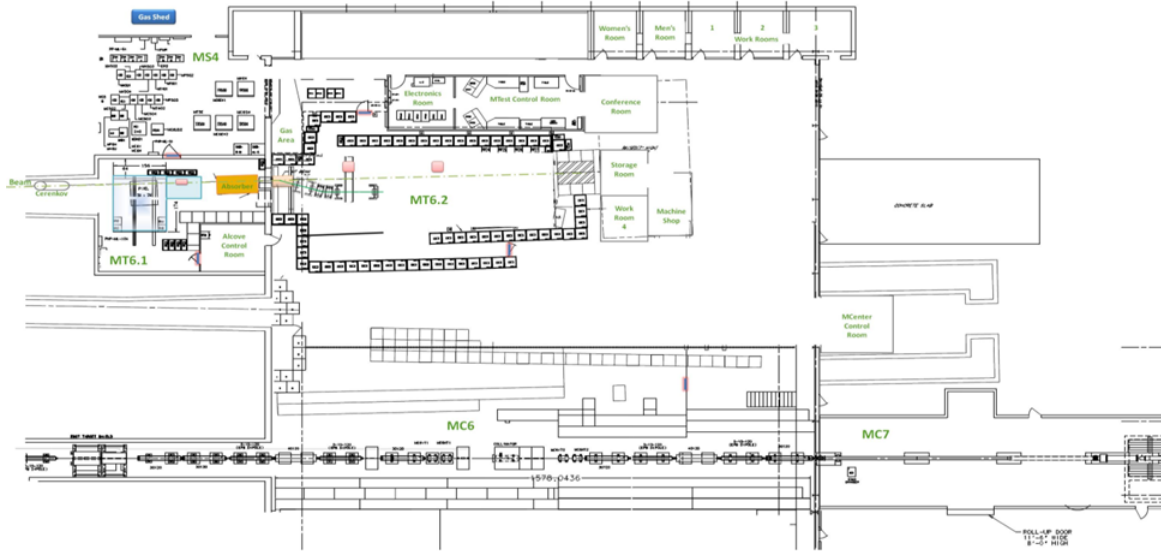


Figure TB-1: View of the Fermilab Test Beam Facility.

Nine new TSWs were approved in FY2014, and 11 new experiments took data during FY 2014. An additional seven experiments returned from previous years to take more data in FY 2014. These 18 experiments are listed in Table TB-I, and represent 321 collaborators from 84 institutions in 20 countries. The chart in Fig. TB-2 shows the growth in these numbers over the last 5 years.

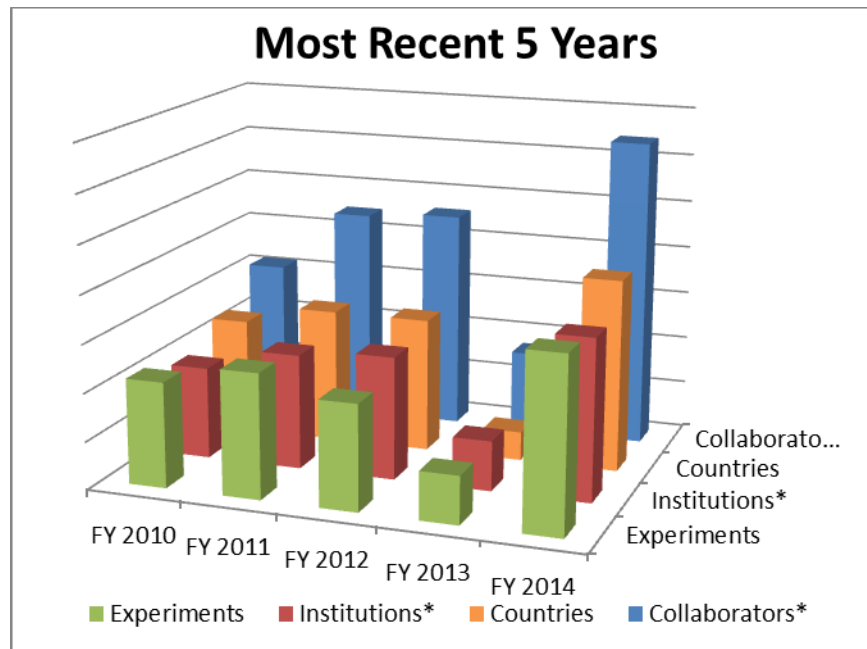


Figure TB-2: Growth in number of experiments, collaborators, institutions and countries served by the FTBF over the past 5 years. \*Number of *Collaborators* has been scaled to fit on plot. \*Number of *Institutions* has been scaled to fit on plot. Note that FY12 consisted of only 7 months of beam and FY13 consisted of only 1 month of beam.

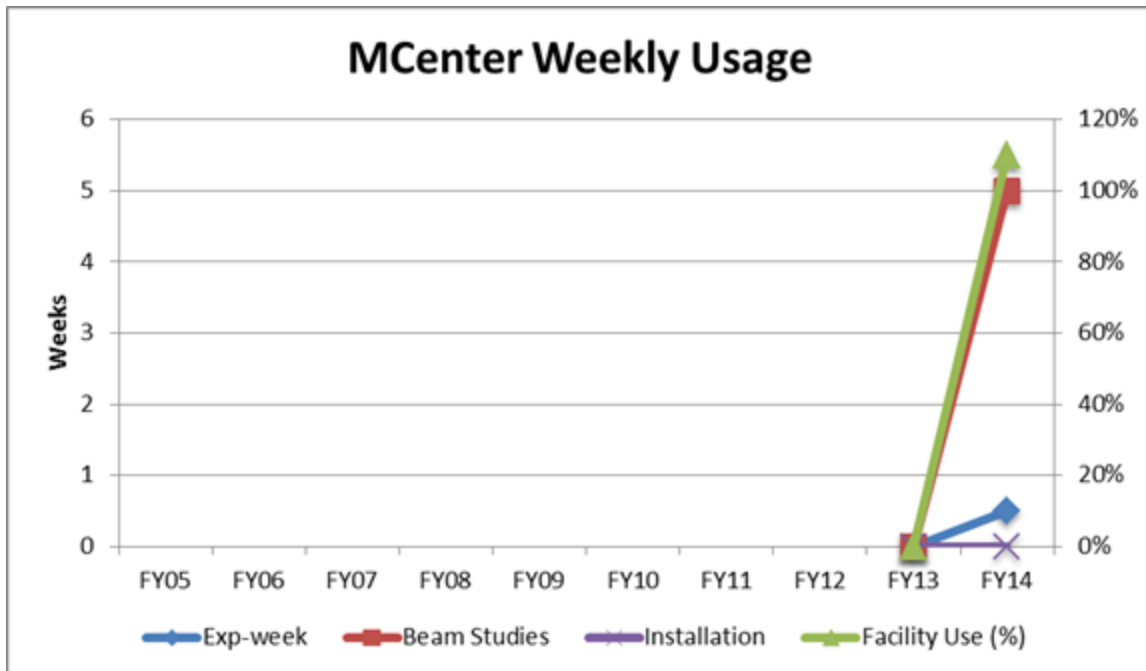
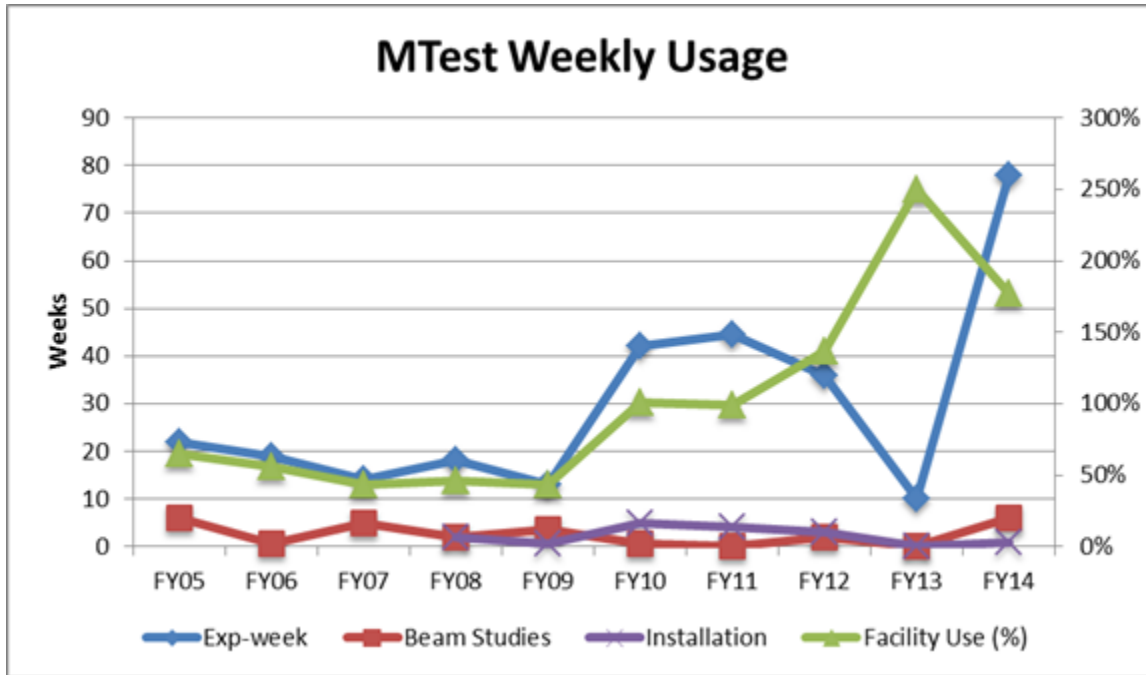


Figure TB-3: Weekly Usage of MTest and MCenter beamlines, nomalized to number of beam-weeks available.

Table TB-I: Test Beam experiments performed in FY 2014.

Test	Description
T1015	Dual Realout Calorimetry
T1018	Spacordian
T1031	ATLAS Tile Electronics Test
T1036	High Rate Pixel Detector for CMS Upgrade
T1037	FIYSUB
T1041	CMS Forward Calorimetry R&D
T1042	Muon g-2 Straw Tracker
T1044	sPHENIX Calorimetry Tests
T1048	PHENIX Fast TOF
T1049	ATLAS large scale Thin Gap Chambers
T1054	sPHENIX PreShower
T1056	ATLAS DBM Module Qualification
T1058	Secondary Emission Calorimeter
T958	FP420 Fast Timing Group
T979	Fast Timing Counters for PSEC
T989	DAMIC
T992	SLHC sensor tests
T994	JASMIN

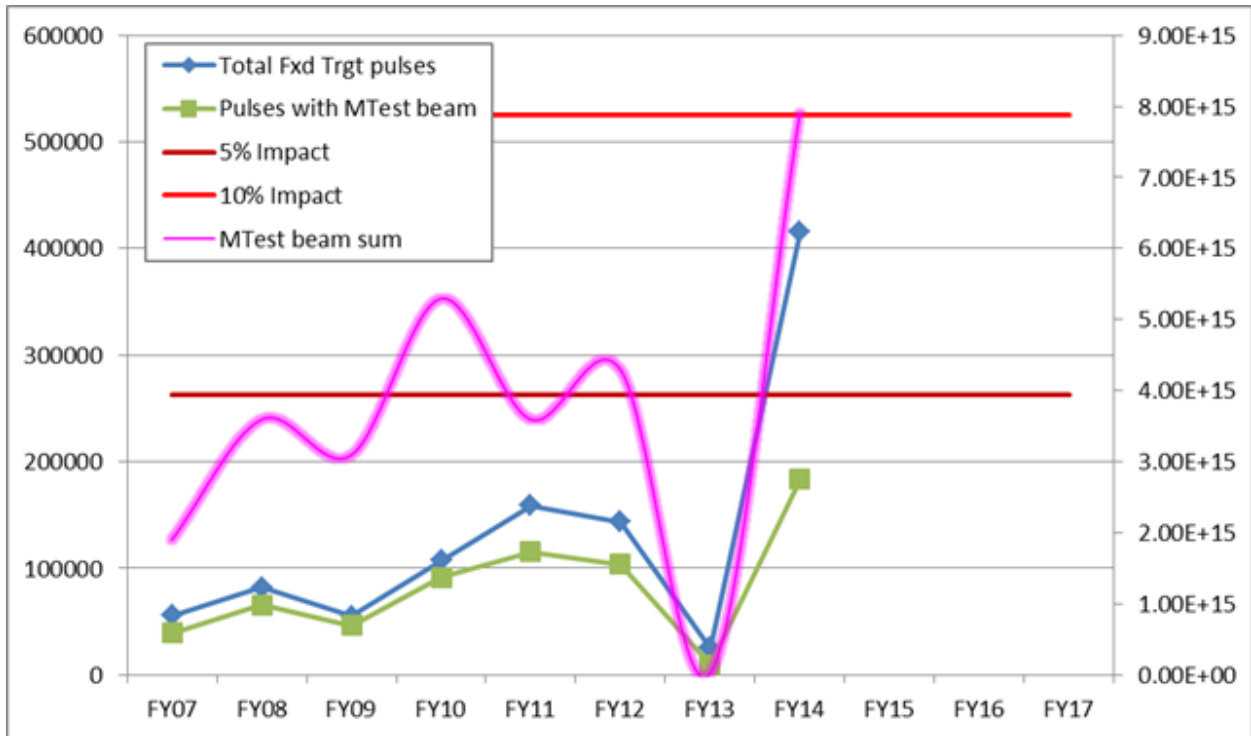


Figure TB-4: Fixed target pulses, to FTBF with and without.

The experiments used the MTest beamline for data taking purposes 177% of the time, for a total of 78 experiment-weeks, out of the 48 weeks with beam available during the year. Weekly facility usage since 2005 (when the facility started taking beam) is shown in Fig. TB-3.

In addition the MCenter beamline was started, and provided beam for 5 weeks, which was used for commissioning the tertiary beamline for the T-1034, LArIAT experiment. This beamline was also used for data taking purposes for half a week by the T-979: Fast Timing Counters for Psec, experiment.

During the 48 weeks of available beam, a total of 415,178 Fixed Target beam cycles occurred, 183,225 of which had beam for the MTest beamline, for a total beam sum of  $7.90 \times 10^{15}$  protons. The MCenter beamline had 16,496 pulses with beam for a total beam sum of  $2.4 \times 10^{16}$  protons.

Until 2012, the Director's guideline for test beam users effect on antiproton production and neutrino beams is 5%, this usually results in one 6 second event in the 60 second timeline for 12 hours a day. However, in 2012 the SeaQuest Experiment started running which was allowed a 10% impact on neutrino beam (one 6 second event /60 seconds for 24 hours a day), and test beam user effects became transparent. The chart shown in Fig. TB-4 shows the number of beam cycles per year over the last 7 years. The impact of FTBF operations has been well below the 5% (now 10%) limit set by the Director.

### **Acknowledgement**

This report gives a brief summary of the performance and output of the accelerator complex and associated accelerator-based experiments during FY14. It therefore summarizes the work of many people from Fermilab and from the collaborating institutions. The credit for the successful outcome of the FY14 running is shared amongst many.